Effect of Mesh Orientation on Accurate Solution in Static Analysis of Composite Plates Structures

Imam Jauhari Maknun
Department of Civil Engineering, Faculty of Engineering, Universitas Indonesia

Andre Yvas
World-Class Research Center “Advanced Digital Technologies”, State Marine Technical University

https://doi.org/10.5109/7326967

出版情報：Evergreen. 11 (4), pp.3325-3332, 2024-12. 九州大学グリーンテクノロジー研究教育センター
バージョン：

Effect of Mesh Orientation on Accurate Solution in Static Analysis of Composite Plates Structures

Imam Jauhari Maknun[1,*], Andre Yvas[2]

[1]Department of Civil Engineering, Faculty of Engineering, Universitas Indonesia, Depok 16424, Indonesia

[2]World-Class Research Center "Advanced Digital Technologies", State Marine Technical University, Saint Petersburg, 190121, Russia

*Author to whom correspondence should be addressed:
E-mail: imam.jm@ui.ac.id

(Received October 21, 2023; Revised July 25, 2024; Accepted November 25, 2024).

Abstract: The mesh orientation effect on the solution accuracy for composite plate structures using the DKMT (Discrete Kirchhoff-Mindlin Triangular) element is evaluated. DKMT is a triangular element that is free of shear locking and shows the best performance in the isotropic and composite plate in thin and thick problems. Two tests proposed with three and nine layers are evaluated using two mesh orientations (right orientation, Mesh A, and left orientation, Mesh B). The convergence of central displacement and total energy is then presented to understand which mesh orientations give better accuracy. The DKMT element gives good convergence behavior to the reference solution. Moreover, the DKMT element is not sensitive to mesh distortion. Mesh A provides better accuracy than mesh B for all cases analyzed in this paper.

Keywords: Composites plates; DKMT; Mesh orientation; Finite Element Method

1. Introduction

Composite materials are widely used in civil, mechanical, and aerospace applications[1-2]. Composite material provides high stiffness and strength-to-weight ratio, corrosion, and high-temperature resistance[3]. An effective computational method in the composite application is very expected since the analytical solutions are only available for simple structures. It is well known that the Finite Element Method performs well in computational mechanics[4]. The composite application can be found in references[5-8]. One of the composite material applications is for plate structures, referred to as bending problems. In the plate bending problem, the Reissner-Mindlin plate is used to formulate many elements capable of being used in thick-to-thin plate structures[9-10].

The phenomenon of shear locking is one of the big problems in finite element analysis for plate-bending elements. The elements often gave poor results in thin plate problems. Reduced and selective integration have been performed to solve the problem[11-14]. They can improve convergence performance, but shear locking still becomes a problem.

Hughes and Tezduyar proposed the Assumed Natural Strain (ANS) as one of the alternatives to solve the shear locking[15-16]. Many authors use it very effectively to develop a new element. Bathe and Dvorkin proposed a variation of the ANS method, and the well-known MITC element was introduced[17-19].

Katili proposed Triangular and Quadrilateral elements called DKMT and DKMQ elements[20-21]. These two elements give good results in thin and thick plates. The result of the thin plate problems proved that these two elements are free of shear locking. The application of DKMQ and DKMT elements in plate and shell for isotropic and composite structures has been presented in literature[22-38]. Regarding the promising results of the DKMT element, it is important to continue studying meshing strategy in composite applications.

The main objective is to demonstrate the effect of mesh orientation on the solution accuracy of the DKMT element in composite applications. In numerical simulation, meshing is one of the important step[39-40], a proper meshing strategy in line with the efficiency and accuracy of numerical simulations. Two numerical tests proposed by Srinivas and Pagano and Hatfield are evaluated by using two different mesh orientations[41-43]. The convergence of central displacement and energy is then presented to understand which mesh orientations give better accuracy.

2. DKMT element

The detailed formulation of the DKMT element in the composite application has been presented in[30,32]. Here, we recall that formulation briefly; the details can be found in references[30,32]. The internal and external energies (Π) of DKMT element are:

$$
\begin{aligned}
&\Pi = \Pi_{int} + \Pi_{ext} \\
&\Pi_{ext} = \int_A w\, f_z\, dA \\
&\Pi_{int} = \Pi_{int}^{b} + \Pi_{int}^{s} \\
&\Pi_{int}^{b} = \frac{1}{2}\int_A \langle \chi \rangle [H_b] \{\chi\}\, dA \qquad \text{(bending energy)} \\
&\Pi_{int}^{s} = \frac{1}{2}\int_A \left(\langle \underline{\gamma} \rangle [H_s] \{\underline{\gamma}\} \right) dA \qquad \text{(shear energy)}
\end{aligned} \tag{1}
$$

Where curvature $\langle \chi \rangle$ is expressed as :

$$
\{\chi\} = \begin{Bmatrix} \beta_{x,x} \\ \beta_{y,y} \\ \beta_{x,y} + \beta_{y,x} \end{Bmatrix} \tag{2}
$$

And $\langle \underline{\gamma} \rangle$ is the transverse shear strain. In this element, the shear strain is interpolated independently. The matrix Hooke's for bending and shear ($[H_b]$,$[H_s]$) are:

$$
[H_b] = \begin{bmatrix} H_{b_{11}} & H_{b_{12}} & H_{b_{13}} \\ & H_{b_{22}} & H_{b_{23}} \\ Sym. & & H_{b_{33}} \end{bmatrix} = \frac{1}{3}\sum_{i=1}^{nl} [H]_i \left(z_{i+1}^3 - z_i^3 \right) \tag{3}
$$

$$
\begin{aligned}
&[H_s] = \begin{bmatrix} \kappa_{11}.\bar{H}_{s_{11}} & \kappa_{12}.\bar{H}_{s_{12}} \\ Sym. & \kappa_{22}.\bar{H}_{s_{22}} \end{bmatrix} \\
&\text{with} \quad [\bar{H}_s] = \begin{bmatrix} \bar{H}_{s_{11}} & \bar{H}_{s_{12}} \\ Sym. & \bar{H}_{s_{22}} \end{bmatrix} = \sum_{i=1}^{nl} [G]_i h_i \quad ; \quad h_i = (z_{i+1} - z_i)
\end{aligned} \tag{4}
$$

where nl is the number of layers, z_i is presented in (Fig. 1) and κ_{11}, κ_{12}, κ_{22} are the shear correction factors.

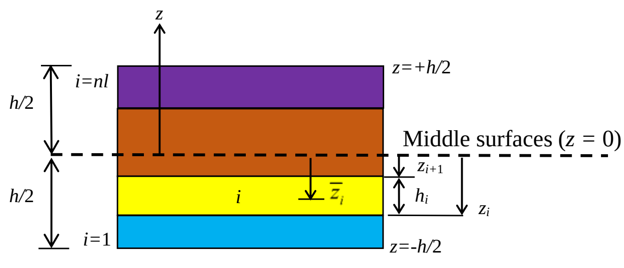

Fig. 1: Layer orthotropic.

DKMT element uses the linear interpolation for transverse displacement (w) and incomplete quadratic interpolation for the rotations (β_x, β_y) as in (Fig. 2):

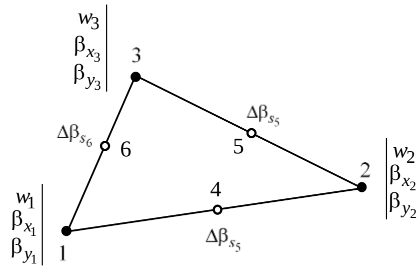

Fig. 2: DKMT Element.

$$
\begin{aligned}
&w = \sum_{i=1,3} N_i\, w_i \\
&\beta_x = \sum_{i=1,3} N_i\, \beta_{xi} + \sum_{k=4,6} P_k\, C_k\, \Delta\beta_{sk} \\
&\beta_y = \sum_{i=1,3} N_i\, \beta_{yi} + \sum_{k=4,6} P_k\, S_k\, \Delta\beta_{sk}
\end{aligned} \tag{5}
$$

N_i and P_k are the linear and quadratic functions, while C_k and S_k are the cosines direction of side k (Fig. 3).

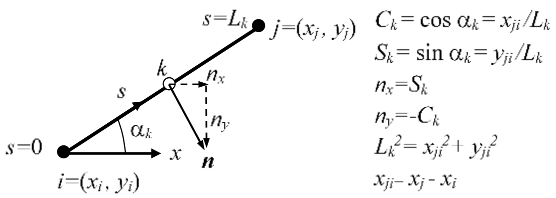

Fig. 3: Geomtery on side k.

We can express equation 2 as:

$$
\{\chi\} = \begin{Bmatrix} \chi_x \\ \chi_y \\ \chi_{xy} \end{Bmatrix} = \begin{Bmatrix} \beta_{x,x} \\ \beta_{y,y} \\ \beta_{x,y} + \beta_{y,x} \end{Bmatrix} = \left[B_{b_\beta} \right] \{u_n\} + \left[B_{b_{\Delta\beta}} \right] \{\Delta\beta_{s_n}\} \tag{6}
$$

Where the linier part of curvature $\left(B_{b_\beta} \right)$ and quadratic part of curvature $\left(B_{b_{\Delta\beta}} \right)$

$$
\left[B_{b_\beta} \right] = \frac{1}{2A} \begin{bmatrix} 0 & -y_{32} & 0 & 0 & -y_{13} & 0 & 0 & -y_{21} & 0 \\ 0 & 0 & x_{32} & 0 & 0 & x_{13} & 0 & 0 & x_{21} \\ 0 & x_{32} & -y_{32} & 0 & x_{13} & -y_{13} & 0 & x_{21} & -y_{21} \end{bmatrix} \tag{7}
$$

$$
\left[B_{b_{\Delta\beta}} \right] = \begin{bmatrix} & P_{k,x}\, C_k & & \\ \ldots & P_{k,y}\, S_k & \ldots & k = 4,5,6 \\ & P_{k,y}\, C_k + P_{k,x}\, S_k & & \end{bmatrix} \tag{8}
$$

$$
P_{k,x} = j_{11} P_{k,\xi} + j_{12} P_{k,\eta} \quad ; \quad P_{k,y} = j_{21} P_{k,\xi} + j_{22} P_{k,\eta}
$$

With

$$
\langle u_n \rangle = \langle w_1 \quad \beta_{x1} \quad \beta_{y1} \quad w_2 \quad \beta_{x2} \quad \beta_{y2} \quad w_3 \quad \beta_{x3} \quad \beta_{y3} \rangle
$$

and $\langle \Delta\beta_{s_n} \rangle = \langle \Delta\beta_{s_4} \quad \Delta\beta_{s_5} \quad \Delta\beta_{s_6} \rangle$ the temporary degrees of freedom at the mid-side nodes that will be eliminated later by using the Discrete Kirchhoff Mindlin method. The independent shear deformation on the side $i-j$:

$$\underline{\gamma}_{s_k} = -\frac{2}{3}\phi_k \Delta\beta_{s_k} \tag{9}$$

$$\phi_k = \left(H^{inv}_{s_{k21}} H_{b_{k32}} + H^{inv}_{s_{k22}} H_{b_{k22}}\right)\left(\frac{12}{L_k^2}\right) \tag{10}$$

where

$$\begin{aligned} \left[H_{b_k}\right] &= \left[R_{k_1}\right]^T \left[H_b\right]\left[R_{k_1}\right] \\ \left[H_{s_k}\right] &= \left[R_{k_2}\right]^T \left[H_s\right]\left[R_{k_2}\right] \\ \left[H^{inv}_{s_k}\right] &= \left[H_{s_k}\right]^{-1} \end{aligned} \tag{11}$$

And L_k is the length of the side k, moreover $\left[R_{k_1}\right]$ and $\left[R_{k_2}\right]$ are given by:

$$\left[R_{k_1}\right] = \begin{bmatrix} S_k^2 & C_k^2 & S_k C_k \\ C_k^2 & S_k^2 & -S_k C_k \\ -2S_k C_k & 2S_k C_k & S_k^2 - C_k^2 \end{bmatrix} \; ; \; \left[R_{k_2}\right] = \begin{bmatrix} S_k & C_k \\ -C_k & S_k \end{bmatrix} \tag{12}$$

The shear strain can be written as :

$$\left\{\underline{\gamma}\right\} = \begin{Bmatrix} \underline{\gamma}_x \\ \underline{\gamma}_y \end{Bmatrix} = \left[B_{s_\gamma}\right]\left[A_\phi\right]\left\{\Delta\beta_{s_n}\right\} \tag{13}$$

$$\left[B_{s_\gamma}\right] = \frac{1}{\det[J]}\begin{bmatrix} -y_{13} & -y_{21} \\ x_{13} & x_{21} \end{bmatrix}\begin{bmatrix} (1-\eta) & -\sqrt{2}\,\eta & \eta \\ \xi & \sqrt{2}\,\xi & (1-\xi) \end{bmatrix}\begin{bmatrix} L_4 & 0 & 0 \\ 0 & \frac{L_5}{\sqrt{2}} & 0 \\ 0 & 0 & -L_6 \end{bmatrix} \tag{14}$$

$$\left[A_\phi\right] = -\frac{2}{3}\begin{bmatrix} \phi_4 & 0 & 0 \\ 0 & \phi_5 & 0 \\ 0 & 0 & \phi_6 \end{bmatrix} \tag{15}$$

By using the Discrete Kirchhoff Mindlin method, we can express :

$$\left\{\Delta\beta_{s_n}\right\} = \left[A_\Delta\right]^{-1}\left[A_u\right]\left\{u_n\right\} \tag{16}$$

With:

$$\left[A_\Delta\right]^{-1} = -\frac{3}{2}\begin{bmatrix} \frac{1}{(1+\phi_4)} & 0 & 0 \\ 0 & \frac{1}{(1+\phi_5)} & 0 \\ 0 & 0 & \frac{1}{(1+\phi_6)} \end{bmatrix} \tag{17}$$

and $[A_u]$ is:

$$\left[A_u\right] = \frac{1}{2}\begin{bmatrix} -\frac{2}{L_4} & C_4 & S_4 & \frac{2}{L_4} & C_4 & S_4 & 0 & 0 & 0 \\ 0 & 0 & 0 & -\frac{2}{L_5} & C_5 & S_5 & \frac{2}{L_5} & C_5 & S_5 \\ \frac{2}{L_6} & C_6 & S_6 & 0 & 0 & 0 & -\frac{2}{L_6} & C_6 & S_6 \end{bmatrix} \tag{18}$$

By introducing equations (17 – 18) into (6), we have :

$$\begin{aligned} \{\chi\} &= \left[B_b\right]\left\{u_n\right\} \\ \left[B_b\right] &= \left[B_{b_\beta}\right] + \left[B_{b_{\Delta\beta}}\right]\left[A_\Delta\right]^{-1}\left[A_u\right] \end{aligned} \tag{19}$$

Then, by introducing equations (17 – 18) into (13), we obtain the assumed shear strain field as:

$$\left\{\underline{\gamma}\right\} = \begin{Bmatrix} \underline{\gamma}_x \\ \underline{\gamma}_y \end{Bmatrix} = \left[B_s\right]\left\{u_n\right\} \; ; \; \left[B_s\right] = \left[B_{s_\gamma}\right]\left[A_{\phi\Delta}\right]\left[A_u\right] \tag{20}$$

and:

$$\left[A_{\phi\Delta}\right] = \left[A_\phi\right]\left[A_\Delta\right]^{-1} = \begin{bmatrix} \frac{\phi_4}{(1+\phi_4)} & 0 & 0 \\ 0 & \frac{\phi_5}{(1+\phi_5)} & 0 \\ 0 & 0 & \frac{\phi_6}{(1+\phi_6)} \end{bmatrix} \tag{21}$$

3. Results and Discussion

To compare the solution accuracy of the DKMT element in a composite plate structure, we analyze 2 cases. The first is a simply supported (SS) sandwich plate proposed by Srinivas, and the second is a three and nine-layer SS plate proposed by Pagano and Hatfield[41-43]. The results of convergence are presented in central displacement and total energy. Two mesh orientations are evaluated to understand the effect of mesh orientation on the accuracy of the solution. The right orientation is Mesh A, and the left orientation is Mesh B.

3.1 Srinivas sandwich plate.

Figure 4 shows the geometric details of the simply supported (SS) sandwich plate proposed by Srinivas[33]. Due to the symmetry condition, only the area of ABCD is analyzed. The details of Mesh A and Mesh B are also presented in Fig.4. The material properties are: E_L =3.4156MPa ; E_T =1.7931MPa ; υ_{LT} = 0.44 ; G_{LT} = 1 MPa ; G_{LZ} = 0.608 MPa ; G_{TZ} = 1.015MPa. The three layers of a 0/0/0 symmetrical sandwich plate with the boundary condition $w = \beta_s = 0$ on the boundary of the plate are evaluated. In this test, we use C = 1, C = 10, and C = 50, where C is the factor proportionality of layer 2 (core) and layers 1 and 3 (skin).

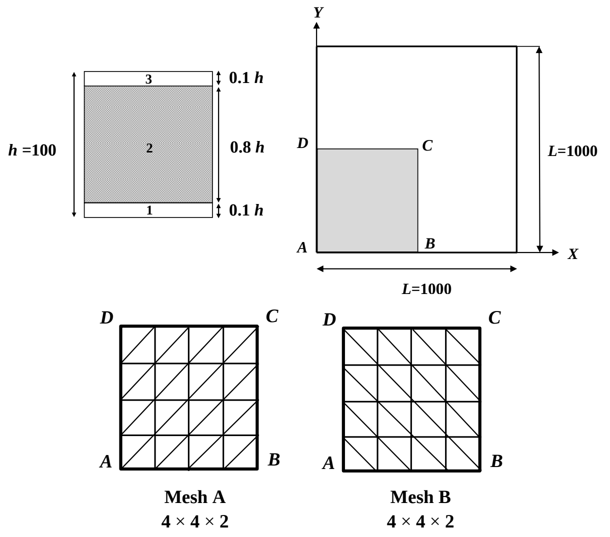

Fig. 4: SS sandwich plate.

The results of the central deflection at point C are presented in Tables 1 and Fig. 5 for two different mesh orientations. The analytical solutions are used as reference solutions[41]. In this test, the central displacement is expressed as :

$$\underline{w}_C = \frac{w_C \, G_{LT}\,(\mathrm{Core})}{h \, f_z} \tag{22}$$

Table 1 and Fig. 5 present the results for uniform mesh. We found the results given by the DKMT element are close to the proposed solution. Also, the results of mesh *A* converge faster than mesh *B* for a small number of elements. To understand the behavior of the whole structure, we also show the results of the total energy of the structure (Fig. 6). Again, we found that mesh *A* performs better than mesh *B*. Starting from 16×16×2 element, mesh A and B give similar results. Mesh A performs better than mesh B for coarse mesh (small number of elements). It is essential to use mesh A for coarse mesh to get accurate results.

Table 1. The Central deflection $\underline{w}_C$.

N×N×2	C = 1		C = 10		C = 50	
	κ11 = κ22 = 0.8333 ; κ2 = 0		κ11 = κ22 = 0.3521 ; κ12 = 0		κ11 = κ22 = 0.0938 ; κ12 = 0	
	MESH A	MESH B	MESH A	MESH B	MESH A	MESH B
4×4×2	180.812	176.221	41.951	40.565	16.935	16.153
8×8×2	181.133	179.921	41.997	41.608	16.880	16.645
16×16×2	181.294	180.975	42.002	41.895	16.853	16.785
32×32×2	181.340	181.258	42.000	41.971	16.843	16.823
64×64×2	181.352	181.330	41.999	41.991	16.839	16.834
Srinivas	181.050		41.910		16.750	

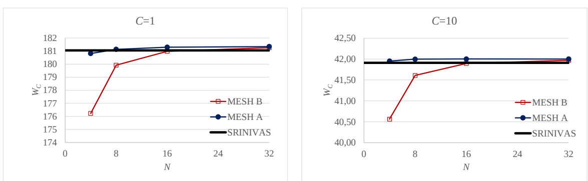

Fig. 5: The central deflection $\underline{w}_C$.

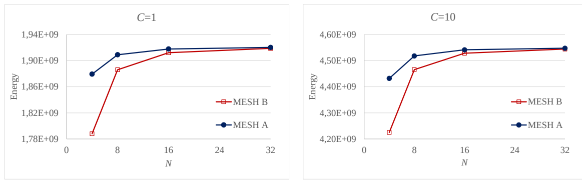

Fig. 6: The convergence of energy with a uniform mesh.

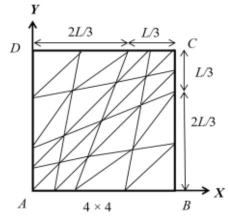

Fig. 7: Distorted mesh for mesh A.

Figure 7 shows the distorted mesh used to analyze the sensitivity of the DKMT element to the element distortion. Table 2 and Fig. 8 present the results for central displacement. The two mesh orientations give the results close to the reference solution. Moreover, we can find again that mesh A performs better than mesh B for a small number of elements. The same behavior is also found in total energy convergence, as presented in Fig. 9. We can conclude that the DKMT element is not sensitive to mesh distortion and gives convergence results as a uniform mesh.

Table 2. The Central deflection $\underline{w}_C$.

N×N×2	C = 1		C = 10		C = 50	
	κ11 = κ22 = 0.8333 ; κ12 = 0		κ11 = κ22 = 0.3521 ; κ12 = 0		κ11 = κ22 = 0.0938 ; κ12 = 0	
	MESH A	MESH B	MESH A	MESH B	MESH A	MESH B
4×4×2	182.311	178.083	42.317	41.171	17.152	16.499
8×8×2	181.404	180.442	42.085	41.773	16.935	16.742
16×16×2	181.341	181.113	42.022	41.939	16.865	16.812
32×32×2	181.350	181.293	42.004	41.983	16.845	16.831
64×64×2	181.354	181.340	42.000	41.994	16.840	16.836
Srinivas	181.050		41.910		16.750	

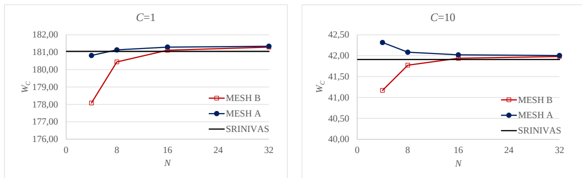

Fig. 8: The central deflection $\underline{w}_C$ distorted mesh.

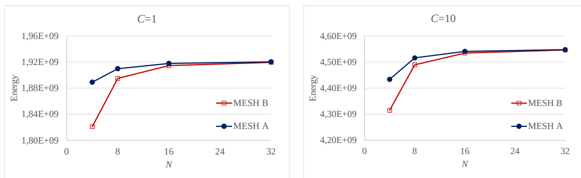

Fig. 9: The convergence of energy with a distorted mesh.

3.2 The 3 and 9 layers SS Plate

Figure 10 presents the details of three and nine-layer square plates proposed by Pagano and Hatfield[42-43]. The uniform and distorted mesh are evaluated by varying *L/h* ratio (*L/h* = 4, 10, 50, 100). The Material properties used in this test are $E_L = 25$ MPa ; $E_T = 1$ MPa ; $\upsilon_{LT} = 0.25$;

G_{LT} = 0.5 MPa ; G_{TZ} = 0.2 MPa. We use shear correction factor for 3 - layer case: κ11 = 0.570 ; κ22 = 0.882 ; κ12 = κ21 = 0 and stratification 0/90/0 symmetrical. While for 9 – layer case, we use κ11 = 0.670 ; κ22 = 0.666 ; κ12 = κ21 = 0 and stratification 0/90/0/90/0/90/0/90/0 symmetrical. The boundary conditions are $w = \beta_s = 0$ on the plate boundary. The sinusoidal loading $f_z = f_0 \sin(\pi x/L)\sin(\pi y/L)$ is applied to the structures. The convergence behavior is presented in the form of vertical displacement in point C, which is expressed as:

$$\underline{w}_C = \frac{\pi^4 w Q}{12 S^4 h\, f_o} \quad ; \quad Q = 4G_{LT} + \left[E_L + E_T\left(1+2\upsilon_{TT}\right)\right]/\left(1-2\upsilon_{LT}\upsilon_{TL}\right) \qquad (23)$$

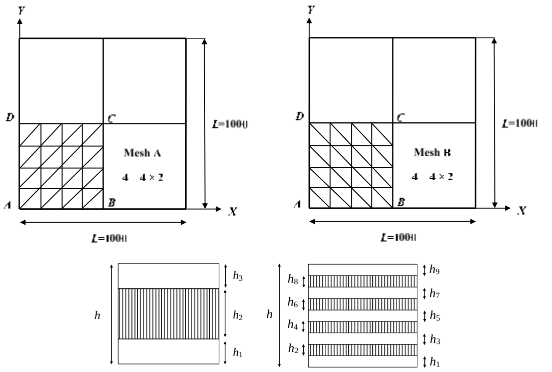

Fig. 10: The 3 and 9 layers.

Table 3. The central deflection $\underline{w}_C$ (3 layers).

N×N×2	3-layer							
	L/h=4		L/h =10		L/h =50		L/h =100	
	MESH A	MESH B	MESH A	MESH B	MESH A	MESH B	MESH A	MESH B
4×4×2	4.746	4.567	1.714	1.667	1.017	0.945	0.997	0.904
8×8×2	4.754	4.744	1.732	1.720	1.024	1.011	1.003	0.957
16×16×2	4.749	4.745	1.737	1.722	1.028	1.018	1.004	1.001
32×32×2	4.747	4.747	1.738	1.728	1.029	1.017	1.005	1.004
64×64×2	4.746	4.746	1.738	1.733	1.030	1.027	1.005	1.005
REF.	4.491		1.709		1.031		1.008	

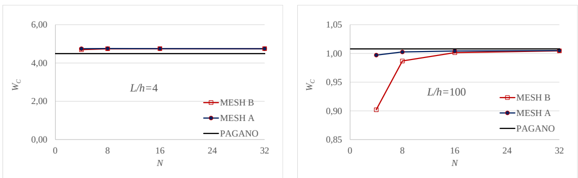

Fig. 11: The central deflection $\underline{w}_C$ (3 layers).

Table 4. The central deflection $\underline{w}_C$ (9 layers).

N×N×2	9-layer							
	L/h = 4		L/h = 10		L/h = 50		L/h = 100	
	MESH A	MESH B	MESH A	MESH B	MESH A	MESH B	MESH A	MESH B
4×4×2	4.210	4.148	1.506	1.446	1.006	0.934	0.991	0.901
8×8×2	4.181	4.158	1.511	1.489	1.015	1.005	1.000	0.974
16×16×2	4.167	4.160	1.511	1.505	1.017	1.012	1.002	0.996
32×32×2	4.162	4.161	1.511	1.508	1.018	1.015	1.002	1.001
64×64×2	4.160	4.160	1.511	1.510	1.018	1.016	1.003	1.001
REF.	4.079		1.512		1.021		1.005	

Table 3 and Table 4 show the results of central displacement for 3-layer and 9-layer cases for different values of *L/h*. We observed that the results were very close to the reference solution. Figure 11 and Fig. 12 present the convergence behavior for *L/h* = 4 and 100. We found that mesh A performs better than mesh B. Mesh A performs better than mesh B for coarse mesh (small number of elements). It is essential to use mesh A for coarse mesh to get accurate results.

Fig. 12: The central deflection $\underline{w}_C$ (9 layers).

Table 5. The central deflection $\underline{w}_C$ (3 layers distorted mesh).

N×N×2	3-layer							
	L/h=4		L/h =10		L/h =50		L/h =100	
	MESH A	MESH B	MESH A	MESH B	MESH A	MESH B	MESH A	MESH B
4×4×2	4.746	4.688	1.714	1.663	1.017	0.951	0.997	0.900
8×8×2	4.754	4.732	1.732	1.723	1.024	1.011	1.003	0.989
16×16×2	4.749	4.737	1.737	1.725	1.028	1.023	1.004	1.001
32×32×2	4.747	4.736	1.738	1.727	1.029	1.024	1.005	1.002
64×64×2	4.746	4.740	1.738	1.728	1.030	1.025	1.005	1.002
REF.	4.491		1.709		1.031		1.008	

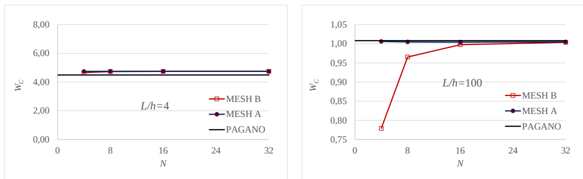

Fig. 13: The central deflection $\underline{w}_C$ (3 layers distorted mesh).

We also perform the test using distorted mesh, presenting the results in Tables 5 – 6 and Fig. 13 – 14. The results are also compared with the solution proposed by Pagano and Hatfield[41-43]. The DKMT element gives good results that converge to the reference solutions for the two mesh orientations. We observe once again that mesh A gives better results than mesh B.

Table 6. The central deflection $\underline{w}_C$ (9 layers distorted mesh).

N×N×2	9-layer							
	L/h = 4		L/h = 10		L/h = 50		L/h = 100	
	MESH A	MESH B	MESH A	MESH B	MESH A	MESH B	MESH A	MESH B
4×4×2	4.210	4.148	1.506	1.458	1.006	0.924	0.991	0.904
8×8×2	4.181	4.158	1.511	1.489	1.015	1.001	1.000	0.988
16×16×2	4.167	4.159	1.511	1.506	1.017	1.008	1.002	0.996
32×32×2	4.162	4.160	1.511	1.509	1.018	1.014	1.002	1.001
64×64×2	4.160	4.160	1.511	1.510	1.018	1.015	1.003	1.001
REF.	4.079		1.512		1.021		1.005	

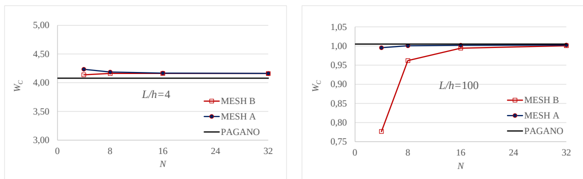

Fig. 14: The central deflection $\underline{w}_C$ (9 layers distorted mesh).

4. Conclusions

The effect of the mesh orientation on the solution accuracy for the DKMT element has been presented in two different directions. The results showed that the DKMT element gives good convergence behavior compared to the reference solution proposed by Srinivas and Pagano & Hatfield. Starting from 8×8×2 element (small number of elements), the results given by DKMT are close to the reference solution. In addition, we found that the DKMT element is not sensitive to mesh distortion. For all tests using distorted mesh, the DKMT element gives convergence results as uniform mesh. Moreover, we found that mesh A performs better than mesh B for coarse mesh (small number of elements). Meshes A and B give similar results when the number of elements increases (starting from 16×16×2). We found that meshing strategy is an essential factor in determining the accuracy of numerical simulation. Finally, the DKMT element can be used as an alternative element to analyze composite plate structures.

Acknowledgments

The financial support from Hibah Publikasi Terindeks Internasional Q2 2022 - 2023 Nomor: NKB-691/UN2.RST/HKP.05.00/2022 is gratefully acknowledged

References

1) S. Nayak and M.P. Kumar,"Mechanical Characterization and Static Analysis of Natural Fiber Based Composite Propeller Blade," *Evergreen*, **10**(2),805-512,(2023). https://doi.org/10.5109/6792832
2) B. Bhati, A. Rath, K. Bector, S.Ahmad, and R. M. Singari, "Recent Developments in the use of Composites for Knee Cap Prosthetics," *Evergreen*, **10**(2),1084-1093,(2023). https://doi.org/10.5109/6793667
3) Q. Li and S. Chen, "A linear smoothed quadratic finite element for buckling analysis of laminated composite plates," *Eng Anal Bound Elem*, **163,** 345–353,(2024) https://doi.org/10.1016/j.enganabound.2024.03.023.
4) L. Huang L, A.H. Sheikh C.T. Ng ,M.C. Griffith, " An efficient finite element model for buckling analysis of grid stiffened laminated composite plates," *Compos Struct*, **122**, 41–50, (2015). https://doi.org/10.1016/j.compstruct.2014.11.039
5) A. Kumar, A.K. Chandra, and S. Angra, " Optimization of Stiffness Properties of Composite Sandwich using Hybrid Taguchi-GRA-PCA," *Evergreen*,**8**(2),310-317,(2021). https://doi.org/10.5109/4480708
6) A. Kumar, A.K. Chandra, and S. Angra, "Numerical Modelling of a Composite Sandwich Structure Having Non Metallic Honeycomb Core," *Evergreen*,**8**(4),759-767,(2021). https://doi.org/10.5109/4742119
7) A. Gupta, H. Kumar, L. Nagdeve, and P. K. Arora," EDM Parametric Study of Composite Materials: A Review,"*Evergreen*,**7**(4),519-529,(2020). https://doi.org/10.5109/4150471
8) A. M. M. Ismaiel, S. M. Metwalli,B. M. N. Elhadidi, and S. Yoshida, "Fatigue Analysis of an Optimized HAWT Composite Blade," *Evergreen*. **4** (2/3), 1-6, (2017). https://doi.org/10.5109/1929656
9) E. Reissner, "The effect of transverse shear deformation on the bending of elastic plates," *Journal of Applied.Mech. in Engineering ASME* ,**12** (2),A69-A77,(1945). https://doi.org/10.1115/1.4009435
10) R.D Mindlin, "Influence of rotator inertia and shear on flexural motion of isotropic elastic plates," *J.Appl.Mech*,**18**,31-38,(1951). https://doi.org/10.1115/1.4010217
11) O.C.Zienkiewicz, R.L Taylor, and J.M.Too, "Reduced integration technique in general analysis of plates and shells," *Int J Numer Methods Eng*, **3**(2), 275–290,(1971). https://doi.org/10.1002/nme.1620030211
12) E.D.L. Pugh, E. Hinton, and O.C. Zienkiewicz, "A study of quadrilateral plate bending elements with 'reduced' integration," *Int J Numer Methods Eng*, **12**(7),1059–1079,(1978). https://doi.org/10.1002/nme.1620120702
13) T.J.R. Hughes, M. Cohen, and M. Haroun, " Reduced and selective integration techniques in the finite element analysis of plates," *Nucl. Eng. Des*, **46**(1),203-222,(1978). https://doi.org/10.1016/0029-5493(78)90184-X
14) D.S. Malkus, and T.J.R. Hughes, "Mixed finite element methods—reduced and selective integration techniques: a unification of concepts," *Comput. Methods Appl. Mech. Eng.*, **15**(1), 63–81, (1978). https://doi.org/10.1016/0045-7825(78)90005-1
15) T.J.R. Hughes, and T.E. Tezduyar, "Finite elements based upon Mindlin plate theory with particular reference to the four-node bilinear isoparametric element," *J. Appl. Mech.*, **48**(3),587–596,(1981). https://doi.org/10.1115/1.3157679
16) R.H. MacNeal, "Derivation of element stiffness matrices by assumed strain distributions," *Nucl. Eng. Des*,**70**(1),3-12,(1982). https://doi.org/10.1016/0029-5493(82)90262-X
17) E.N. Dvorkin, and K.J. Bathe, "A continuum mechanics based four-node shell element for general non-linear analysis," *Eng. Comput.*, **1**(1), 77-88, (1984). https://doi.org/10.1108/eb023562
18) K.J.Bathe, and E.N. Dvorkin, " A formulation of general shell elements—the use of mixed interpolation of tensorial components," *Int J Numer Methods Eng*, **22**(3), 697–722,(1986). https://doi.org/10.1002/nme.1620220312
19) K.J.Bathe, and E.N. Dvorkin, "A four-node plate bending element based on Mindlin-Reissner plate theory and a mixed interpolation," *Int J Numer Methods Eng*, **21**, 367-383, (1985). https://doi.org/10.1002/nme.1620210213
20) I. Katili, " A new discrete Kirchhoff-Mindlin element based on Mindlin-Reissner plate theory and assumed shear strain fields- part I: An extended DKT

element for thick-plate bending analysis," *Int J Numer Methods Eng*, **36**, 1859-1883, (1993). https://doi.org/10.1002/nme.1620361106

21) I. Katili, " A new discrete Kirchhoff-Mindlin element based on Mindlin-Reissner plate theory and assumed shear strain fields- part II: An extended DKQ element for thick plate bending analysis," *Int J Numer Methods Eng*, **36**, 1885-1908, (1993). https://doi.org/10.1002/nme.1620361106
22) I. Katili, I.J. Maknun, O. Millet, and A . Hamdouni, "Application of DKMQ element for composite plate bending structures," *Compos Struct*,**132**, 166 – 174,(2015). https://doi.org/10.1016/j.compstruct.2015.04.051
23) I.,Katili, J.L.Batoz, I.J.Maknun, A. Hamdouni, and O.Millet,"The Development of DKMQ Plate Bending Element for Thick to Thin Shell Analysis Based on Naghdi/Reissner/Mindlin Shell Theory," *Finite Elem Anal Des*, **100**, 12-27, (2014). https://doi.org/10.1016/j.finel.2015.02.005
24) I. Katili, J.L Batoz, I.J.Maknun, and P.Lardeur, "A comparative formulation of DKMQ, DSQ and MITC4 quadrilateral plate elements with new numerical results based on s-norm tests," *Comput. Struct.*,**204**,48-64,(2018a). https://doi.org/10.1016/j.compstruc.2018.04.001
25) I.J.Maknun,I. Katili, O. Millet, and A. Hamdouni, " Application of DKMQ24 shell element for twist of thin-walled beams: comparison with Vlasov theory," *Int. J. Comput. Methods Eng. Sci. Mech.*, **17** (6), 391-400,(2016). https://doi.org/10.1080/15502287.2016.1231240
26) H. Irpanni,I.Katili, and I.J.Maknun, "Development DKMQ Shell Element with Five Degrees of Freedom per Nodal," *Int. J. Mech. Eng. Robot. Res*, **6**,248-252,(2017). https://doi.org/ 10.18178/ijmerr.6.3.248-252
27) I. Katili, I.J.Maknun, J.L. Batoz, and A. Ibrahimbegović, "Shear deformable shell element DKMQ24 for composite structures," *Compos Struct*, **202**,182–200,(2018b). https://doi.org/10.1016/j.compstruct.2018.01.043
28) I. Katili, I.J.Maknun, E.Tjahjono and I. Alisjahbana, "Error estimation for the DKMQ24 shell element using various recovery methods," *Int. J. Technol*, **6** , 1060-1069,(2017). https://doi.org/10.14716/ijtech.v8i6.699
29) A.M. Katili, I.J. Maknun, and I. Katili, "Theoretical equivalence and numerical performance of T3s and MITC3 plate finite elements," *Struct Eng Mech*, **69**(5),527-536,(2018c). https://doi.org/10.12989/sem.2019.69.5.527
30) I. Katili, I.J. Maknun, J.L. Batoz, and A.M. Katili, "Asymptotic equivalence of DKMT and MITC3 elements for thick composite plate," *Compos Struct*, **206**,363–379,(2018d). https://doi.org/10.1016/j.compstruct.2018.08.017
31) I. Katili, I.J. Maknun, A.M. Katili, S.P.A. Bordas, and S.Natarajan, "A unified polygonal locking-free thin/thick smoothed plate element," *Compos Struct*,**219**,147-157(2019a). https://doi.org/10.1016/j.compstruct.2019.03.020
32) I. Katili, I.J.Maknun,J.L. Batoz, and A.M. Katili, "A comparative formulation of T3γs , DST, DKMT and MITC3+ triangular plate elements with new numerical results based on s-norm tests," Eur. J. Mech. A/Solids, **78**,103826, (2019b). https://doi.org/10.1016/j.euromechsol.2019.103826
33) I.J.Maknun,I. Katili, A. Ibrahimbegović, and A.M. Katili, "A new triangular shell element for composites accounting for shear deformation," *Compos Struct*, **243**, 112214 (2020). https://doi.org/10.1016/j.compstruct.2020.112214
34) I.J.Maknun, I. Katili, and H. Purnomo, "Development of DKMT element for error estimation in composite plate structures," *Int. J. Technol*, **6** (5), 780 -789 (2015). https://doi.org/10.14716/ijtech.v6i5.1050
35) I.J. Maknun and S., Zarfatina, "Shear Correction Factor Effects on Functionally Graded Materials (FGMs) Beams using Discrete Shear Gap (DSG) Element," Int. J. Technol, **12**(6), 1250–1260, (2021). https://doi.org/10.14716/ijtech.v12i6.5210.
36) I. Katili, J.L. Batoz, I.J. Maknun, and A.M. Katili, "On static and free vibration analysis of FGM plates using an efficient quadrilateral finite element based on DSPM," *Compos Struct*, **261**, 113514, (2021). https://doi.org/10.1016/j.compstruct.2020.113514.
37) I.J., Maknun, S.Natarajan, and I. Katili, " Application of discrete shear quadrilateral element for static bending, free vibration and buckling analysis of functionally graded material plate," *Compos Struct*, **284**, 115130, (2022). https://doi.org/10.1016/j.compstruct.2021.115130
38) I. Katili, J.L. Batoz, S Bouabdallah, I.J. Maknun, and A.M.Katili, "Discrete shear projection method for mechanical buckling analysis of FGM sandwich plates," *Compos Struct*, **312**, 116825, (2023) https://doi.org/10.1016/j.compstruct.2023.116825
39) M.K. Thompson, , J. M. Thompson, "ANSYS Mechanical APDL for Finite Element Analysis," (2017). https://doi.org/10.1016/B978-0-12-812981-4.00006-X
40) J. Tang, P. Cui, B. Li, Y. Zhang, H. Si, "Parallel hybrid mesh adaptation by refinement and coarsening," *Graph. Models*, **111**, 101084, (2020) https://doi.org/10.1016/j.gmod.2020.101084
41) Srinivas, S., "A Refined analysis of composite laminates," *J Sound Vib*, **30** (4), 495–507 (1973). https://doi.org/10.1016/S0022-460X(73)80170-1
42) N.J.Pagano, "Exact solutions for rectangular bidirectional composites and sandwich plates," *J Compos Mater*, **4**(1),20–34,(1970). https://doi.org/10.1177/002199837000400102

43) N.J. Pagano, and S.J. Hatfield, "Elastic behavior of multilayered bidirectional composites," *AIAAJ*, **10**(7),931–933,(1972). https://doi.org/10.2514/3.50249